

# A Technique for the Fullwave Automatic Synthesis of Waveguide Components: Application to Fixed Phase Shifters

Ferdinando Alessandri, *Member, IEEE*, Mauro Mongiardo, *Member, IEEE*, and Roberto Sorrentino, *Fellow, IEEE*

**Abstract**—An efficient computer synthesis technique for waveguide components, based on rigorous field-theoretical models, has been developed. A computer code has been specifically set up for the automatic design of fixed phase shifters in rectangular waveguide technology. Only the electrical specifications are required to generate, normally in 15 to 20 minutes on a 386/16 MHz IBM PC, the geometrical structure of the components. The agreement with the experiments is shown to be so accurate as to avoid any tuning of the circuits realized.

The efficiency and accuracy of the code is based on i) a suitable segmentation technique of the microwave structure to obtain a very simple but rigorous network model; ii) the efficient representation of the modal series for the electromagnetic fields; iii) a synthesis procedure based on a simplified model to obtain a good initial guess for the final full-wave optimization routine.

## I. INTRODUCTION

THE computer-aided design (CAD) of microwave circuits consists basically of the following phases: i) modeling, ii) analysis, and iii) optimization [1]. Though distinct, the three phases are strictly interlaced. For example, the optimization consists of a number of repeated analyses, according to some strategy. The iterative process is terminated successfully when the circuit specifications are met.

The overall efficiency of the CAD procedure depends on the efficiencies of the single phases and must be evaluated in view of the entire fabrication process. The accuracy of the model thus its reliability, in fact, influences the efficiency, since it makes it possible to simplify or even avoid costly and time consuming experimental work. On the other hand, as the accuracy of the model is improved, the associated computational (and analytical) effort is normally increased also. As optimization usually requires hundreds or thousands iterations, one is normally forced by limited computer capabilities to employ relatively simple, thus approximate, models.

On the other hand, many applications require extremely accurate design capabilities to minimize costs of manu-

facturing, to determine the effects of mechanical tolerances, to predict the effects of imperfections in the fabrication process, etc. This is not only true in the area of (M)MIC's, but also in the more conventional area of waveguide circuits. A typical example is that of space applications. Sophisticated antenna performances of modern satellite communication systems involve the design of quite complex microwave networks with very strict requirements [2].

In spite of the considerable developments of computing resources in recent years, progress has still to be made to improve the computational efficiency of the theoretical models for microwave structures. Very accurate models are required that, at the same time, involve relatively modest computer expenditures.

This paper is aimed to give a contribution in this direction. An efficient computer synthesis technique for waveguide components, based on rigorous field-theoretical models, has been developed. A computer code has been specifically set up for the automatic design of fixed phase shifters. Only the input electrical specifications are required to generate the geometrical structure of the circuits. The agreement with the experiments is such as to avoid any tuning of the circuits realized.

An initial guess for the waveguide phase shifter geometry is first determined by synthesizing an approximate but still rather accurate model. The accurate choice of the initial guess is of great importance in determining the efficiency (and the success) of the final optimization. The latter is based on a full-wave but numerically simple model to adjust the geometry to the final dimensions.

The model adopted is based on the application of the microwave network formalism in conjunction with a suitable segmentation of the microwave structure into rectangular cells. Employing extremely efficient representations of the modal series for calculating the generalized admittance matrices of the cells, simple analysis procedures for even complex waveguide structures are obtained.

The synthesis technique can be applied not only to other waveguide components, such as filters, couplers, etc., but can also be extended, with proper modifications, to MIC circuits. The case of microstrip circuits, however, can be made much simpler than the waveguide case by adopting the planar circuit approach [3], thus a 2-dimensional magnetic wall model. In such a case, because of the modified

Manuscript received August 26, 1991; revised February 7, 1992.

F. Alessandri was with Microdesign S.a.s., Via Magliano Sabina 39, I-00199, Rome, Italy. He is presently with the Istituto di Elettronica, Università di Perugia, I-06100, Perugia, Italy.

M. Mongiardo is with the Dipartimento di Ingegneria Elettronica, Università di Roma, "Tor Vergata," I-00173, Rome, Italy.

R. Sorrentino is with the Istituto di Elettronica, Università di Perugia, I-06100, Perugia, Italy.

IEEE Log Number 9200461.

boundary conditions, the impedance matrix is to be used instead of the admittance matrix.

Segmentation is a common procedure in any computer analysis of microwave structures with complex geometries [4], [5]. For totally irregular shapes only strictly numerical methods such as Finite Difference or Finite Element methods can be applied. In many practical cases, however, irregular shapes can be subdivided into simple rectangular geometries. These cases lend themselves to the application of mode-matching (MM) techniques, which are particularly suited in rectangular coordinates. The way the segmentation procedure is applied, however, affects the efficiency of the resulting computer code. One type of segmentation can result in an analysis procedure one order of magnitude faster than another. Some ideas on efficient segmentation techniques have been presented in [6] for the case of multiport branch-guide couplers and are reviewed in Section II for the case of stub-loaded rectangular waveguides. This is, in fact, the structure chosen for the realization of fixed phase shifters [7], [8]. In Section III-A, the generalized admittance matrix of microwave circuits is formulated in terms of the dyadic Green's function.

Besides the efficiency of the model, the efficiency of the analysis depends on the representation of the electromagnetic fields in the structure. Actually, certain efforts have been made in the literature to increase the efficiency of the MM technique by suitably accounting for edge singularities [9]–[12]. This can be done by adopting proper singular basis functions for expanding the field quantities at the diaphragm or step edges. In this paper, however, the MM method is applied in a slightly unconventional form, the fields being expanded in terms of cavity modal series. Fast convergent series expressions are obtained by choosing the proper Green's function representation. Although, in principle, the same technique as in [11], [12] could be applied, this would lead to a quite involved mathematical treatment, with questionable numerical advantages. The discussion on the field modal series and the use of the various Green's function expressions, specialized to the case of E-plane waveguide structures, is presented in Section III-B. A comparison of the various formulations in terms of numerical efficiency is given in Section III-C. The specific synthesis procedure for waveguide stub loaded phase shifter is illustrated in Section IV, while theoretical and experimental results are presented in the last Section.

## II. SEGMENTATION TECHNIQUES FOR THE MICROWAVE NETWORK MODELING OF WAVEGUIDE COMPONENTS

The mode-matching method is based on the expansion of the electromagnetic (EM) field in a waveguide in terms of its normal modes. The boundary conditions at a junction between different waveguides lead to a linear system of equations in the expansion coefficients. By virtue of the equivalence between guided modes and transmission lines, the microwave network formalism can be devel-

oped, where each mode is represented by a transmission line. Systems of equations in the modal expansion coefficients at the junctions are represented by generalized multiport networks, where each electrical port corresponds to a given mode. In a similar and more general fashion, any microwave circuit can be represented by a generalized multiport networks. Here we recall that a microwave circuit is *a region enclosed by metallic walls of any shape and communicating with the exterior only by way of a number of transmission lines or waveguides, which may be called the terminals of the circuit*. [13].

With the application of the microwave network formalism, the analysis of a complex microwave structure is reduced to that of the overall equivalent network resulting from the connection of its constituent elements. These are junctions, waveguide sections and microwave circuits (in the sense already specified).

Among the efforts to improve the efficiency of the mode-matching method, not much attention has been devoted to reducing the complexity of the overall equivalent circuit by identifying the most suitable segmentation of the structure. Actually, when designing components with complicated geometries and a great number of junctions, computer time can be reduced by even one order of magnitude by selecting the proper segmentation technique.

The point will be illustrated at the example of the structure of Fig. 1(a), which represents a phase shifter [7] consisting of a rectangular waveguide section loaded with a number  $N_s = 4$  of E-plane stubs. The presence of H-plane discontinuities [8] is not considered for the moment. The structure can be regarded also as the cascade of  $2N_s = 8$  waveguide discontinuities of alternating enlargement- and reduction-type. Note that Fig. 1(a) can also represent a waveguide filter.

Conventionally, the analysis strategy, which is the basis for the Generalized Scattering Method (GSM) [14], consists of associating a generalized multiport network to each discontinuity, then analyzing the resulting equivalent network, Fig. 1(b). The computer effort for one complete analysis involves  $4N_s - 1 = 15$  matrix inversions. The S-matrix of each step, in fact, requires one matrix inversion for its computation. The size of the matrix to be inverted equals the number of modes at the narrow side of the junction. Seven additional inversion are required to compute the cascade connection of the 8 S-matrices of the model of Fig. 1(b).

A more advantageous procedure consists of viewing Fig. 1(a) as consisting of 4 cells (or cavities) (regions 1, 3, 5 and 7) connected by 3 waveguide sections. This is obtained by grouping together one enlargement-type with the successive reduction-type step. Each cell constitutes a microwave circuit that can be represented by a multiport network. The overall equivalent circuit is shown in Fig. 1(c). This segmentation has been called the *cellular segmentation* [6]. The numerical advantage is actually greater than one could imagine by comparing at a first glance Fig. 1(c) and (b).

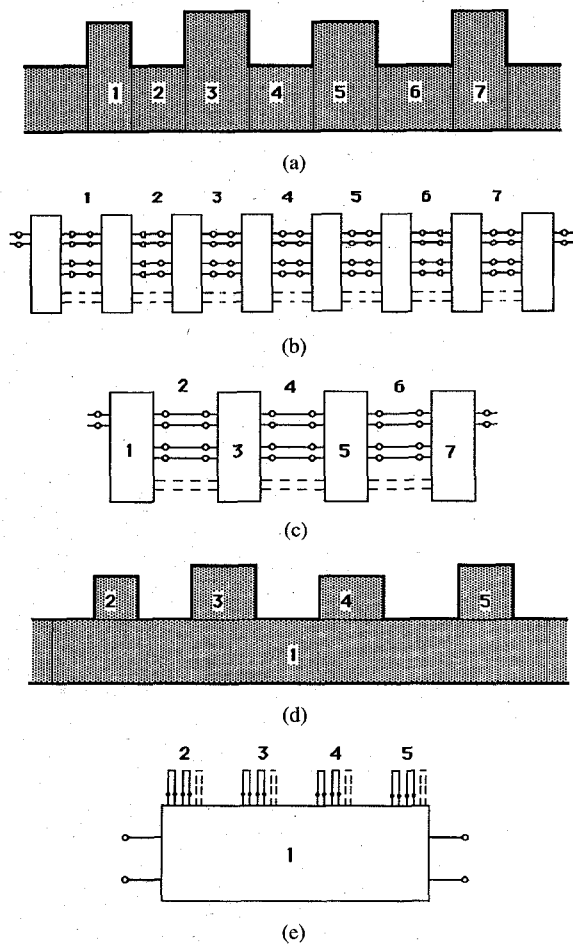


Fig. 1. (a) Schematic of waveguide structure with E-plane steps for the realization of fixed phase shifter [7]. (b) Generalized equivalent circuit of Fig. 1(a) using the conventional Generalized Scattering Method. Steps are represented by multiport networks connected by uniform transmission lines. (c) Generalized equivalent circuit of Fig. 1(a) using the cellular segmentation technique (CST). Cells are represented by multiport networks connected by uniform transmission lines. (d) Another cellular segmentation ("transverse segmentation") of Fig. 1(a). (e) Generalized equivalent circuit of Fig. 1(a) using the segmentation of Fig. 1(d).

In fact, as has been proved in [6] and will be shown in the next section, the multiport network model of each cell does not require any matrix inversion if the admittance matrix representation is adopted, while only one inversion would be necessary for the scattering matrix computation. As a consequence, the total number of matrix inversions for the circuit of Fig. 1(c) is equal to the number of waveguide sections connecting the stubs, thus only  $N_s - 1 = 3$ .

The idea of segmenting the geometry into cells instead of discontinuities and waveguide sections therefore reduces substantially the complexity of the overall equivalent circuit; in conjunction with the admittance matrix representation a notable further computational advantage is obtained. A special case of cellular segmentation can be applied to the geometry of Fig. 1(a) when, as is usually the case, the waveguide height ' $b$ ' is constant throughout the length of the phase shifter. This implies that regions

2, 4, 6 have the same height as the input and output waveguides. A further reduction of the computer expenditure is achieved by the segmentation shown in Fig. 1(d). The entire waveguide length is seen as a cavity with six outputs, four being terminated by shorted stubs. The remaining outputs are placed far enough from the stubs so that all higher order modes have died out. In this manner, after removing all internal ports between the cavity and the stubs, the Y-matrix of the cavity is reduced to the  $2 \times 2$  admittance matrix of the whole structure. This segmentation corresponds to the so called transverse segmentation technique (TST) [6]. The equivalent circuit corresponding to Fig. 1(d) is shown in Fig. 1(e). All connecting waveguide lengths are eliminated, the circuit consisting only of the equivalent networks of the cells.

One additional aspect concerning the numerical efficiency of the segmentation is the number of ports of the various elements. It is known that MM exhibits the relative convergence phenomenon, so that, generally speaking, the number of ports is higher the wider the size of the connection. It turns out, in particular, that the TST (Fig. 1(e)) is especially convenient over both the cellular segmentation (Fig. 1(c)) and, particularly, the GSM, when the stubs are long and narrow. In such a case a high number of ports are required in Fig. 1(c), while a few ports are necessary for Fig. 1(e).

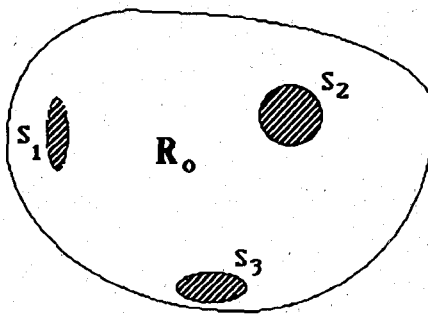
In conclusion, the waveguide structure of Fig. 1(a) can be more efficiently modeled using the admittance matrix representation and adopting the segmentation scheme of Fig. 1(e). In this manner only one matrix inversion is necessary. On the contrary, the use of the conventional generalized scattering matrix for each step, would require 15 matrix inversions.

### III. COMPUTATION OF THE GENERALIZED ADMITTANCE MATRIX

The segmentation procedure described in the previous Section determines a simple circuit topology (Fig. 1(e)) where the admittance matrices of the cells constituting the waveguide structure have to be evaluated. The field theoretical procedure for the efficient computation of the constituent Y-matrices is described in this Section. The procedure is especially efficient for the Y-matrix. When preferred, the scattering matrix can be evaluated from the admittance matrix using standard formulas.

#### A. Generalized Admittance Matrix of a Cavity: Formulation of the Problem

Consider first an arbitrary microwave circuit  $R_o$  enclosed by a perfectly conducting surface  $S$  where  $N_p$  physical outputs  $S_i$  (Fig. 2) are produced. The EM field in  $R_o$  is determined uniquely by the knowledge of the tangential electric field over the output  $S_i$ . By slightly modifying the treatment in [16], the magnetic field in  $R_o$  can be ex-

Fig. 2. A microwave network with  $N_p = 3$  outputs.

pressed as

$$\begin{aligned} \mathbf{H}(\mathbf{r}) &= j\omega\epsilon \oint_S \mathbf{n} \times \mathbf{E}(\mathbf{r}') \cdot \underline{\mathbf{G}}(\mathbf{r}, \mathbf{r}') dS' \\ &= j\omega\epsilon \sum_{i=1}^{N_p} \int_{S_i} \mathbf{n} \times \mathbf{E}(\mathbf{r}') \cdot \underline{\mathbf{G}}(\mathbf{r}, \mathbf{r}') dS' \end{aligned} \quad (1)$$

the integral over  $S$  being reduced to the only portions  $S_i$ , where  $\mathbf{n} \times \mathbf{E}$  is not zero. In (1) the quantity  $\mathbf{n} \times \mathbf{E}$  can be interpreted as a magnetic surface current flowing on  $S_i$ .  $\underline{\mathbf{G}}$  is the dyadic Green's function for the magnetic field in  $R_o$ . It is a solution of

$$\nabla \times \nabla \times \underline{\mathbf{G}} - k^2 \underline{\mathbf{G}} = \underline{\mathbf{I}} \delta(\mathbf{r} - \mathbf{r}') \quad \text{in } R_o \quad (2)$$

$$\mathbf{n} \times \nabla \times \underline{\mathbf{G}} = 0 \quad \text{on } S \quad (2')$$

where  $k^2 = \omega^2 \mu \epsilon$ ,  $\underline{\mathbf{I}}$  is the unit dyadic,  $\delta$  is the Dirac delta function.

The relationships among field quantities at the openings  $S_i$  can be formulated in terms of a generalized admittance matrix by expanding the tangential  $\mathbf{E}$ - and  $\mathbf{H}$ -fields into a suitable set of vector basis functions

$$\mathbf{n} \times \mathbf{E}^{(i)} = \sum_{k=1}^{N_i} V_k^{(i)} \phi_k^{(i)} \quad (3a)$$

$$\mathbf{H}^{(i)} = \sum_{k=1}^{N_i} I_k^{(i)} \phi_k^{(i)}, \quad (3b)$$

$N_i$  being the number of basis functions taken into account on  $S_i$ . The vector basis functions in (3a) and (3b) need not to be the same, but this choice leads to a Galerkin-type procedure having variational properties. The  $\phi_k^{(i)}$ 's can be any complete orthonormalized set of vector basis functions. They are chosen, as usual, as the modal eigenvectors of a waveguide having  $S_i$  as the cross section. The series in (3a, b) are truncated to  $N_i$  terms for numerical reasons.

The expansion coefficient  $V_k^{(i)}$  and  $I_k^{(i)}$  represent the equivalent voltage and current on the  $k$ th electrical port on the output  $S_i$ . They are related to the respective field quantities on  $S_i$  by

$$V_k^{(i)} = \int_{S_i} \mathbf{n} \times \mathbf{E}(\mathbf{r}) \cdot \phi_k^{(i)}(\mathbf{r}) dr \quad (4a)$$

$$I_k^{(i)} = \int_{S_i} \mathbf{H}(\mathbf{r}) \cdot \phi_k^{(i)}(\mathbf{r}) dr \quad (4b)$$

Combining (4b) with (1) and (3a) we obtain

$$I_m^{(j)} = \sum_{i=1}^{N_p} \sum_{k=1}^{N_i} Y_{mk}^{(ji)} V_k^{(i)} \quad (5)$$

where

$$Y_{mk}^{(ji)} = \int_{S_j} \int_{S_i} \phi_m^{(j)}(\mathbf{r}) \cdot \underline{\mathbf{G}}(\mathbf{r}, \mathbf{r}') \cdot \phi_k^{(i)}(\mathbf{r}') dr dr' \quad (6)$$

defines the generalized admittance matrix of  $R_o$ . This quantity represents the amplitude of the  $m$ th current component entering the  $j$ th opening produced by a unit  $k$ th component of the voltage at the  $i$ th opening, all the other voltage components being zero.

As already pointed out in [19] no matrix inversion is necessary to compute the generalized admittance matrix. This is due to the fact that the admittance matrix is the natural representation of a cavity with conducting walls. When a magnetic wall model is adopted for microstrip circuit, the impedance matrix is the most efficient network representation.

The drawback with the  $Y$ -matrix is that it possesses polar singularities (see (A2) in the appendix), thus numerical overflow may occur occasionally. In the computations made for present study, however, such an event has never been observed.

When the cavity has only one opening, as is the case of the stub regions 2, ..., 5 of Fig. 1(d), expression (6) holds for  $i = j = 1$  only.

At the connection between two cells, say cells 1 and 2 of Fig. 1(d), it is easily seen that the continuity of the magnetic field is equivalent, in network terms, to the direct connection between the corresponding ports of the equivalent networks.

### B. Green's Function Representations for Rectangular Cells

Once the general expression (6) for the generalized admittance matrix has been derived, we obtain now the expression for the Green's function relevant to the present problem. We will refer to a rectangular cell such as cell No. 1 of Fig. 1(d), the specialization to the stub cells being straightforward. For clarity, the geometry is sketched in Fig. 3. Outputs No. 1 and  $N$  are placed along the  $y$ -axis and correspond to the output ports of the structure, while outputs 2 to  $N - 1$  are to be connected to the stubs.

With respect to the general case, a basic simplification is obtained since the structure of Fig. 1(d) is uniform in the  $x$ -direction and the EM field is excited by the dominant  $TE_{10}$  modes incident from the input waveguides. The  $x$ -dependence is therefore determined by  $\sin(\pi x/a)$ , or  $\cos(\pi x/a)$  depending on the field component, and no  $x$ -component for the electric field exists. The EM field in each cell can be described by means of a scalar magnetic potential (LSE modes), or equivalently in terms of the  $H_x$  component. In practice, the computation of the dyadic Green's function is reduced to the  $G_{xx}$  component only.

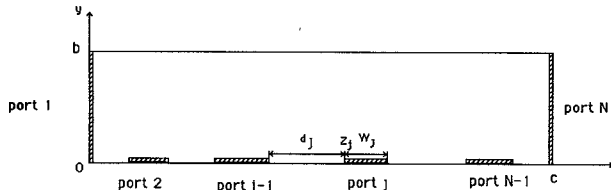


Fig. 3. Side-view of a rectangular resonator corresponding to cell 1 of Fig. 1(d), where outputs ports 2 through  $N - 1$  are connected to short circuited stubs.

Renaming  $G_{xx}$  simply as  $G$ , and dropping the  $x$ -dependence, the differential problem (2) becomes

$$\nabla^2 G + k^2 G = \delta(y - y') \delta(z - z') \quad (7)$$

with homogeneous Neumann boundary condition

$$\frac{\partial G}{\partial n} = 0 \quad \text{on } S. \quad (7')$$

In (7)  $k'^2 = k^2 - (\pi/a)^2$ , 'a' being the cell size in the  $x$ -direction, and

$$\nabla^2 = \frac{\partial^2}{\partial y^2} + \frac{\partial^2}{\partial z^2}.$$

For a rectangular cell of sizes  $b$  and  $c$  along the  $y$  and  $z$ -directions respectively, the Green's function can be obtained in terms of resonant modes [15]. The resulting expression is

$$_o G(y; z, y', z') = \sum_{m=0}^{\infty} \sum_{n=0}^{\infty} \frac{\xi_{mn}(y, z) \xi_{mn}(y', z')}{k'^2 - \left(\frac{m\pi}{b}\right)^2 - \left(\frac{n\pi}{c}\right)^2} \quad (8)$$

where  $\xi_{mn}(y, z)$  are the eigenmodes of the cell:

$$\xi_{mn} = \sqrt{\frac{\epsilon_m \epsilon_n}{bc}} \cos \frac{m\pi y}{b} \cos \frac{n\pi z}{c}, \quad (9)$$

$\epsilon_m = 1$  for  $m = 0$ ,  $\epsilon_m = 2$  for  $m \neq 0$ .  $G(y, z; y', z')$  represents the magnetic field distribution  $H_x(y, z)$  due to a unit pulse of electric field  $E_y(y', z')$  or, equivalently, to a unit pulse of magnetic current  $M_x(y', z')$ .

A considerably more efficient way to express the Green's function of our rectangular cell consists of replacing the double series over  $(m, n)$  in (8) with a single series over  $m$  or  $n$ . This can be done by expressing the EM field in terms of *waveguide* modes instead of *cavity* modes. Two convenient alternative expressions can be obtained (see [20]) depending on whether the  $y$ - or  $z$ -direction is taken as the propagation direction. For propagation in the  $z$ -direction one obtains

$$_z G = \sum_m f_m(y) f_m(y') \frac{\cos k_{zm} z_< \cos k_{zm} (c - z_>)}{k_{zm} \sin k_{zm} c} \quad (10)$$

with

$$z_< = \begin{cases} z' & z > z' \\ z & z < z' \end{cases} \quad z_> = \begin{cases} z & z > z' \\ z' & z < z' \end{cases}$$

where  $k_{zm}^2 = k'^2 - k_{ym}^2$  and  $k_{ym} = m\pi/b$  and

$$f_m(y) = \sqrt{\frac{\epsilon_m}{b}} \cos \frac{m\pi}{b} y.$$

Similarly, for propagation in the  $y$ -direction the following expression for the Green's function is obtained

$$_y G = \sum_m g_m(z) g_m(z') \frac{\cos k_{ym} y_< \cos k_{ym} (b - y_>)}{k_{ym} \sin k_{ym} b}$$

$$g_m(z) = \sqrt{\frac{\epsilon_n}{c}} \cos \frac{n\pi}{c} z \quad (11)$$

where  $k_{ym}^2 = k'^2 - k_{zm}^2$  and  $k_{zm} = m\pi/c$ .

### C. Numerical Efficiency of the Various Representations

The numerical advantage of using a single instead of a double series needs not to be stressed. The present approach should not be confused with that in [21], where *two* modal series are replaced by *one*.

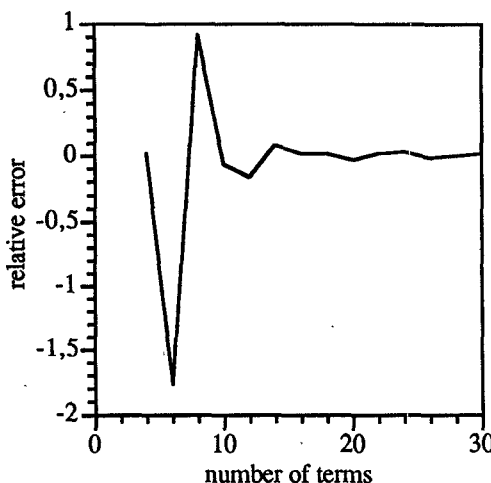
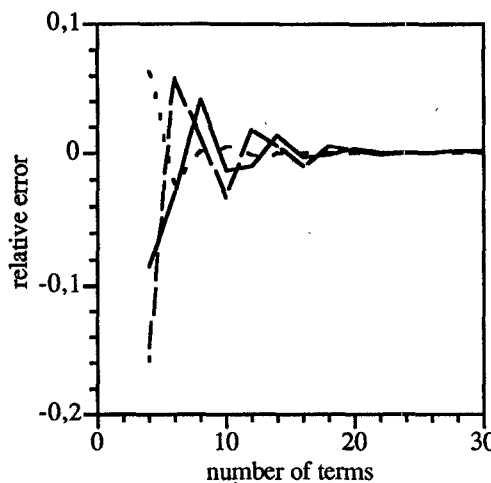
The choice between the two alternative expressions (10) or (11) for  $G$  ultimately depends on the convergence of the resultant series for the generalized  $Y$ -matrix of the cell (see Appendix). In practice, the numerical advantage of using  $_z G$  or  $_y G$  is determined by the locations of the ports and on the sizes of the cell.

In order to illustrate this point, we have computed the various expressions for the generalized  $Y$ -matrix of a rectangular cell  $b \times c$  ( $b = 9.52$  mm,  $c = 37$  mm). For analogy with the notation adopted for the Green's function expressions, we will denote the  $Y$ -matrix expressions with the symbols  $_o Y$ ,  $_z Y$ , or  $_y Y$  depending on whether expression (8), (10) or (11) for  $G$  is employed. The magnetic field eigenvectors of normal modes of rectangular waveguides have been used as vector basis functions  $\phi_k$ . They are given in the Appendix along with the admittance matrix elements.

Let us first observe that, since port 1 extends to the entire  $b$  size of the cell, the series for  $_z Y_{mn}^{(i,1)}$  reduce to a single term, and provides therefore the most efficient expression. This is due to the fact that the expanding functions  $\phi_k$  on the outputs have been selected as the normal modes of the corresponding waveguide. For the same reason, the double series for  $_y Y_{mn}^{(i,1)}$  reduces to a single series that coincides with  $_y Y_{mn}^{(i,1)}$ .

To give an idea of the convergence behavior of such series, Fig. 4 shows the relative error pertaining to the series for  $_o Y_{11}^{(2,1)}$  or, equivalently  $_y Y_{11}^{(2,1)}$ , while the convergence behaviors of the series for  $_y Y_{21}^{(2,1)}$ ,  $_y Y_{11}^{(3,1)}$ ,  $_y Y_{21}^{(3,1)}$  is shown in Fig. 5 for a distance  $d_2 = 10$  mm and for  $w_2 = 4.5$  mm between the two outputs. Note that different vertical scales have been used in these, as well as in the following figures.

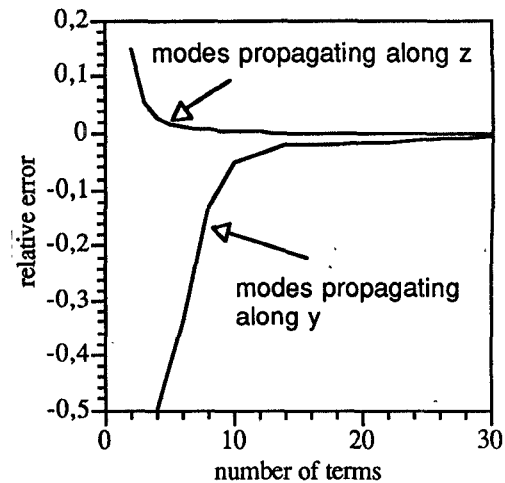
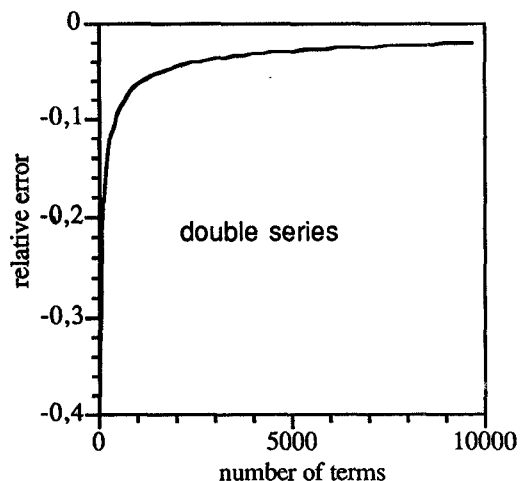
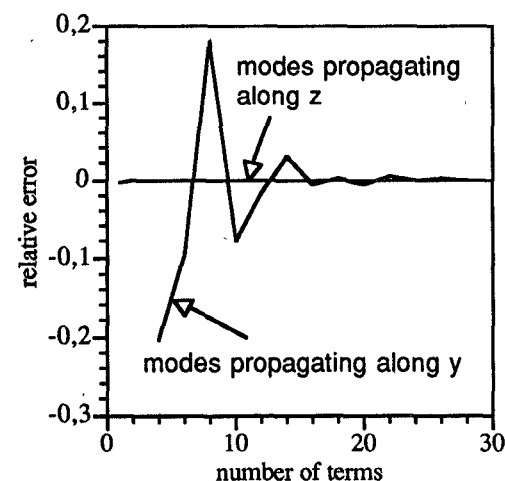
In spite of the good convergence behaviors shown in Figs. 4 and 5, the series (10) is obviously to be preferred as it provides the correct value with just one term.

Fig. 4. Convergence behavior of the mutual admittance  ${}_0 Y_{11}^{(2,1)}$  or  ${}_y Y_{11}^{(2,1)}$ .Fig. 5. Convergence of the mutual admittances between perpendicular outputs:  ${}_y Y_{21}^{(2,1)}$  (---),  ${}_y Y_{11}^{(3,1)}$  (- - -),  ${}_y Y_{21}^{(2,2)}$  (—).

Let us now examine the element  $Y_{11}^{(2,2)}$  which corresponds to the self-admittance of the dominant mode at output 2 ( $w_2 = 4.5$  mm), i.e., the input admittance seen at output 2 by the dominant mode when all the other outputs are shorted. The convergence behaviors of  ${}_z Y_{11}^{(2,2)}$  and  ${}_y Y_{11}^{(2,2)}$  are shown in Fig. 6, while that of the double series  ${}_0 Y_{11}^{(2,2)}$  is plotted in Fig. 7.

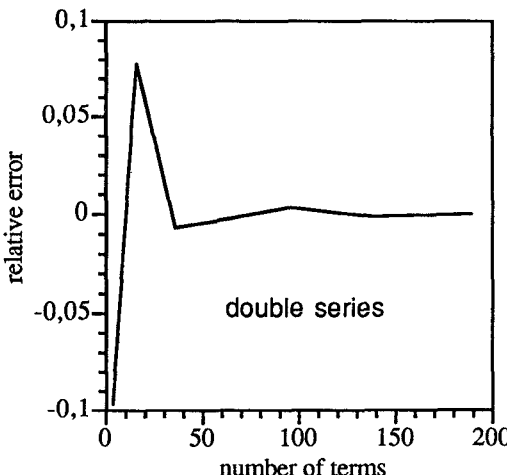
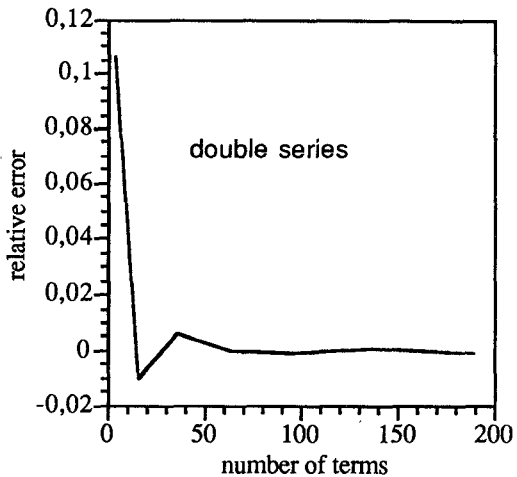
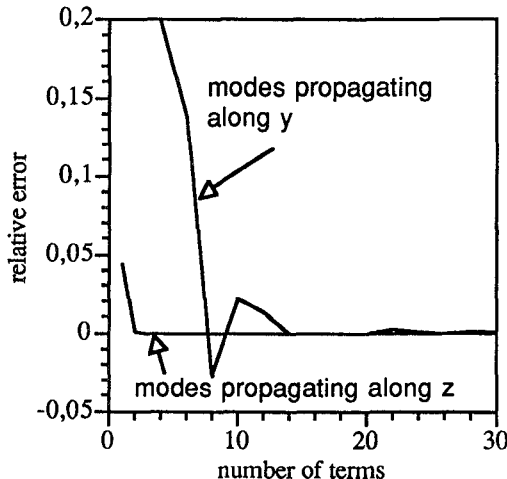
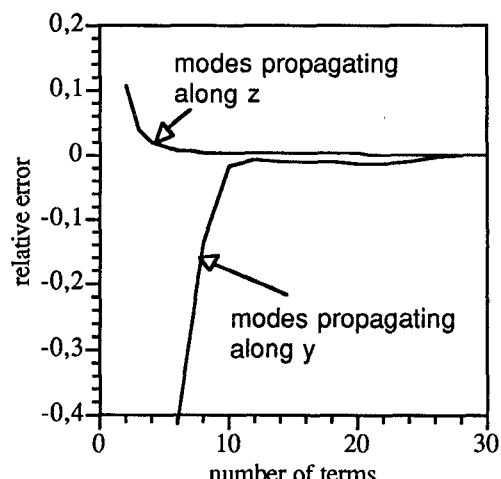
For a given accuracy (e.g., a relative error of 1%), the numerical effort associated with the computation of  ${}_0 Y_{11}^{(2,2)}$  is extremely higher (almost 1000 times) than with the single series (10) or (11).

It should be noted that the computation of the self-admittance is the most cumbersome from a numerical point of view. For the trans-admittances seen at same physical port (e.g., output 2), but between different modes (i.e. using different expanding and testing functions  $m \neq k$  in (6)), the convergence is much faster. This is shown, for example, in Fig. 8 for  ${}_z Y_{12}^{(2,2)}$  and  ${}_y Y_{12}^{(2,2)}$  and Fig. 9, for the double series  ${}_0 Y_{12}^{(2,2)}$ . To get an accuracy of the order of 1%, the double series requires approximately 40 terms,

Fig. 6. Convergence behaviors of the series  ${}_z Y_{11}^{(2,2)}$  and  ${}_y Y_{11}^{(2,2)}$ .Fig. 7. Convergence behavior of the double series  ${}_0 Y_{11}^{(2,2)}$ .Fig. 8. Convergence behavior of  ${}_z Y_{12}^{(2,2)}$  and  ${}_y Y_{12}^{(2,2)}$ .

16 terms are required for  ${}_y Y_{12}^{(2,2)}$ , while only 2 terms are enough for  ${}_z Y_{12}^{(2,2)}$ .

In the evaluation of the trans-admittances between different physical ports, such as outputs 2 and 3, different

Fig. 9. Convergence behavior of  $o Y_{12}^{(2,2)}$ .Fig. 11. Convergence of  $o Y_{11}^{(2,3)}$  for distance between port 2 and port 3  $d_3 = 8$  mm.Fig. 10. Convergence of  $z Y_{11}^{(2,3)}$  and  $y Y_{11}^{(2,3)}$  for  $d_3 = 8$  mm.Fig. 12. Same as Fig. 10 except with  $d_3 = 1$  mm.

rates of convergence are expected depending on the distance between the outputs. In particular, when modes propagating along  $z$  are used, only one or two terms are expected to be necessary to achieve very accurate results. This is confirmed by Fig. 10, showing the convergence behaviors of the series  $z Y_{11}^{(2,3)}$  and  $y Y_{11}^{(2,3)}$  for the trans-admittance between the dominant modes at outputs 2 and 3  $Y_{11}^{(2,3)}$ . The convergence behavior of  $o Y_{11}^{(2,3)}$  is shown in Fig. 11. Both Figs have been plotted for a distance  $d_3 = 8$  mm between output 2 and 3. Only two terms for  $z Y_{11}^{(2,3)}$  are sufficient to get an almost exact result.

When outputs 2 and 3 are put to a very close distance  $d_3 = 1$  mm, the convergence rate is lower for all series, as shown in Fig. 12. In any case, the series involving modes propagating in the  $z$ -direction always exhibits the highest convergence rate, providing very accurate results with no more than 5 terms.

In summary, the adoption of proper field expansions in the evaluation of the scalar Green's functions make it possible to evaluate almost analytically the generalized admittance matrices of the rectangular cells into which waveguide components, and specifically the phase shifter

sketched in Fig. 1(d), can be segmented. In most cases, in fact, the  $Y$ -matrix elements expansions can be reduced to just one term. In the examples examined, the worst case is that of the self admittances which require up to 6 terms to get an error less than 1%.

#### IV. SYNTHESIS OF WAVEGUIDE PHASE SHIFTER

In the previous Sections rigorous field-theoretical tools for very fast and accurate computer analyses of waveguide components have been described. The theory has been presented for the case of E-plane waveguide structures. In this case the EM fields can be described in terms of LSE<sup>(x)</sup> modes only, but the same principles apply to cases when both E- and H-plane discontinuities are present.

This section is devoted to the specific application developed, i.e., to the automatic synthesis of waveguide phase shifters. Such components are typically employed in antenna beam-forming networks. Requirements in terms of wide band and compact design are very strict. Automatic design tools which can avoid costly experimental work are of paramount importance.

An effective technique for realizing waveguide fixed phase shifters consists of loading a waveguide section with a number of stubs.

A rigorous field-theory CAD of stub-loaded phase-shifter has recently been presented by Dittloff *et al.* [7]. One limitation of their procedure is that the required phase shift is obtained with reference to a waveguide section of proper length. To allow the differential phase shift to be achieved with respect to a waveguide of the same length, the 'a' dimension of the waveguide phase shifter was introduced in [8] as an additional degree of freedom.

The simultaneous use of stub-loading and cutoff shifting to attain better phase shift characteristics can be qualitatively explained by the following arguments.

Basically, a fixed phase shifter is required to produce in a given frequency range a constant phase shift  $\Delta\phi_o$  with respect to a reference transmission line length. The ideal phase delay response is obtained by a simple shift of that of the reference line.

In order to approximate the ideal response one could change the broader 'a' side of the rectangular waveguide, thus shifting the cutoff frequency. This, however, would have also the effect of changing the slope of the phase response, which would become lower if the cutoff is lowered.

It can be shown that an opposite effect is obtained by periodically loading the waveguide with a series inductance realized by short E-plane stubs. The resultant periodic structure has, in a passband, a steeper phase delay slope. By suitably combining the two effects it is possible to design extremely compact broad band phase shifters. Of course, other solutions are possible, e.g., using capacitive instead of inductive loads.

In both [7] and [8] an optimization procedure is employed for the design. Unless a good initial guess is available, the optimization procedure can be extremely computer intensive or even ineffective. A good initial guess can be obtained by first synthesizing a periodical structure. This procedure was shortly described in [17] and is recalled below in a somewhat modified form. For the sake of simplicity, the synthesis of the initial guess structure is described in terms of an equivalent transmission line model, where discontinuity effects are neglected. In practice, the synthesis can be done (see below) using a waveguide model for the periodic structure including most of such effects.

Let  $\phi_{\text{ref}}(f)$  be the phase delay of the reference waveguide,  $\Delta\phi_o$  the required constant phase shift. In a frequency range  $[f_1, f_2]$  the phase response  $\phi_p$  of the phase shifter must be

$$\phi_p(f) = \phi_{\text{ref}}(f) + \Delta\phi_o. \quad (12)$$

An additional constraint to be usually imposed on the phase shifter is that its length must be shorter than the reference waveguide by a prescribed amount  $\Delta L$ .

The phase constant of the reference line is

$$\phi_{\text{ref}}(f) = \beta_{\text{ref}}(f)(L + \Delta L) \quad (13)$$

where  $\beta_{\text{ref}}(f)$  is the phase constant of the reference line and  $L$  is the length of the phase shifter\*. The synthesis of the phase shifter can be made in terms of an equivalent transmission line section of the same length, which produces the same phase shift in the same frequency range. Let  $\beta_p(f)$  be the phase constant of the equivalent transmission line, then its phase delay is

$$\phi_p(f) = \beta_p(f)L. \quad (14)$$

Combining (12)–(14), the phase constant  $\beta_p$  is obtained as a function of the specification (12) and the length  $L$  of the phase shifter:

$$\beta_p(f) = \beta_{\text{ref}}(f)(1 + \Delta L/L) + \Delta\phi_o/L. \quad (15)$$

Observe that while  $\Delta L$  is always a positive quantity,  $\Delta\phi_o$  may be either positive or negative. As a consequence,  $\beta_p$  can be either greater or smaller than  $\beta_{\text{ref}}$ .

The above equation (15) defines the synthesis problem for the equivalent transmission line section. The required phase constant behavior  $\beta_p(f)$  can be approximated in the frequency range  $[f_1, f_2]$  by that of a periodic structure composed of alternating reactances  $X$  and transmission line sections of characteristic impedance  $Z_l$  and phase constant  $\beta_l$  (Fig. 13(a)). The reactances are realized with shorted stubs of lengths  $d_s$ , characteristic impedance  $Z_s$  and same phase constant  $\beta_l$ .

To reduce mismatchings, a convenient choice for the cell length  $d$  was found to be a quarter wavelength of the periodic structure at center frequency  $f_o = (f_2 + f_1)/2$ , thus

$$d = \pi/(2\beta_{po}) \quad (16)$$

where we have put for simplicity  $\beta_{po} = \beta_p(f_o)$ . This assumption makes it possible to determine the total length of the equivalent transmission line, i.e., the phase shifter length, for any given number  $N$  of cells. Since  $L = Nd$ , combining (16) and (15), one obtains

$$L = \frac{1}{\beta_{\text{ref},o}} \left( \frac{N\pi}{2} - \beta_{\text{ref},o}\Delta L - \Delta\phi_o \right). \quad (17)$$

The required phase constant  $\beta_p(f)$  is thus fully determined in the whole band by (17) and (15). Incidentally, it can be observed that (17) establishes a minimum number of cells  $N$  for the physical realizability ( $L > 0$ ).

From the theory of periodic structures [18], the following relation is obtained for the periodic structure of Fig. 13(b):

$$\frac{Z_s}{Z_1} \tan(\beta_1 d_s) = 2 \frac{\cos(\beta_1 d) - \cos(\beta_p d)}{\sin(\beta_1 d)} \quad (18)$$

where the phase constant of the periodic structure has been assumed to be the same as the ideal value  $\beta_p$ .

\*Observe that the length  $(L + \Delta L)$  of the reference line must be a positive quantity for the phase shifter to be realizable. For a zero length reference line, in fact, a frequency independent phase shift  $\phi_p(f) = \Delta\phi_o$  would result, implying an infinite group velocity.

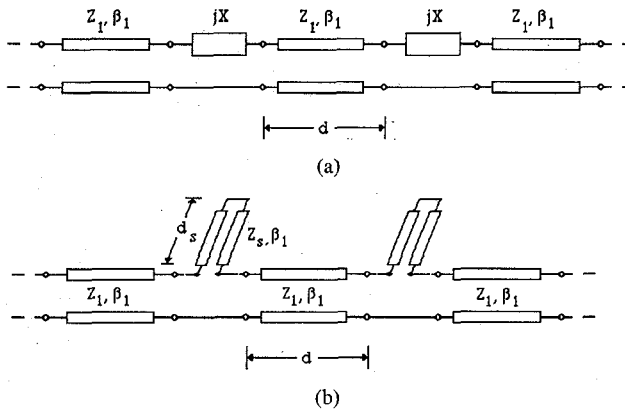


Fig. 13. Periodic transmission line (a) and its realization with distributed elements (b).

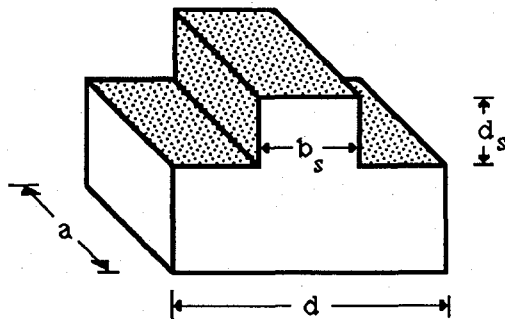


Fig. 14. Elementary cell of the waveguide phase shifter.

Equation (18) cannot be satisfied but approximately. The three unknown quantities, namely the normalized characteristic impedance of the stub ( $Z_s/Z_l$ ), the stub length ( $d_s$ ) and the phase constant of the line sections ( $\beta_l$ ), can be determined by a simple optimization procedure to minimize the quadratic error in the operating frequency band. The initial guess for the number  $N$  of cell is increased until the input requirements are met.

The synthesized transmission line model of the phase shifter is then easily translated into a waveguide model consisting of the connection of  $N$  elementary cells, such that depicted in Fig. 14. Because of the dispersive character of the waveguide, the transformation is made at center frequency. Observe that the phase constant  $\beta_l$  of the transmission lines of Fig. 13 determines the broader 'a' size, thus the cutoff frequency, of the waveguide structure. Since the phase shifter has normally to be connected to a reference waveguide, two H-plane steps at the ends of the phase shifter must be introduced.

The structure synthesized by the above procedure provides the starting point for the final optimization routine of the phase shifter. Optimization must be applied in order to compensate for discontinuity effects not included in the simplified transmission line model and to minimize the insertion loss of the device.

The synthesis procedure described for the transmission line model can actually be applied directly to the waveguide structure, i.e. using the full-wave model to synthesize the waveguide cell of Fig. 14. There is, in fact, a

correspondence between the four parameters ( $d$ ,  $d_s$ ,  $Z_s/Z_l$  and  $\beta_l$ ) of the transmission line cell (Fig. 13) and the four geometrical parameters ( $d$ ,  $d_s$ ,  $b_s$  and  $a$ ) of the waveguide cell (Fig. 14). This is actually the procedure that has been followed. With such a procedure, most discontinuity effects, i.e. those due to higher order mode insertion within the single waveguide cell, are already taken into account in the synthesis procedure, which thus provides an even better starting point for the final optimization.

## V. COMPUTED AND EXPERIMENTAL RESULTS

Sophisticated phase shifters can be designed automatically with modest computer resources (a 386 IBM PC is sufficient) by the full-wave synthesis technique described in the previous Sections. The design input data are used to generate first a periodically loaded waveguide section. This is the initial guess for the subsequent optimization routine where the terminal H-plane steps are included. A gradient-based (quasi-Newton) optimization routine has been used.

The theoretical and measured responses of a 9-stub phase shifter, designed in the band 10.95–12.75 GHz, are shown in Fig. 15. The phase shifter was designed to produce a differential phase shift of  $\Delta\phi = -85^\circ$  with respect to a reference waveguide length  $\Delta L = 37.04$  mm shorter. With the notation of Fig. 16, the dimensions of the device are quoted in Table I. Note that the width 'a' of the phase shifter is different from the standard dimension of the waveguide (as a consequence of  $\beta_l$  being different from  $\beta_{ref}$ ).

To give an idea of the numerical accuracy of the various approaches discussed in this paper, the theoretical responses in Fig. 15 have been computed using the three representations of Section III, i.e. using  $z$ - and  $y$ -propagating modes as well as resonant modes.

All results are in close agreement, particularly, at lower frequency. The small disagreement observed (particularly for the phase at high frequencies) is due to the truncations in the Green's functions series and to the limited number of basis functions on the outputs (only 3 in all cases). In particular, the resonant mode expansion is estimated to be slightly less accurate. Better agreements at the expense of CPU time could be achieved increasing the number of basis functions. As far as the computer time is concerned, considerable differences are found. In order to generate the data plotted in Fig. 15, the use of the double series requires approximately one hour and a half, while only 2 minutes are required using the single series relative to modes propagating along  $z$ .

Because of the good initial guess, the whole optimization routine requires only twenty minutes on a IBM 386 PC-16 MHz.

Equivalent electrical characteristics are exhibited by the phase shifter of Fig. 17, although it is made of only 6 instead of 9 stubs. This improvement is due to having adopted a structure with symmetrical double-stubs. Symmetry reduces the effects of higher order modes. The geometry of the modified phase shifter is quoted in Table II.

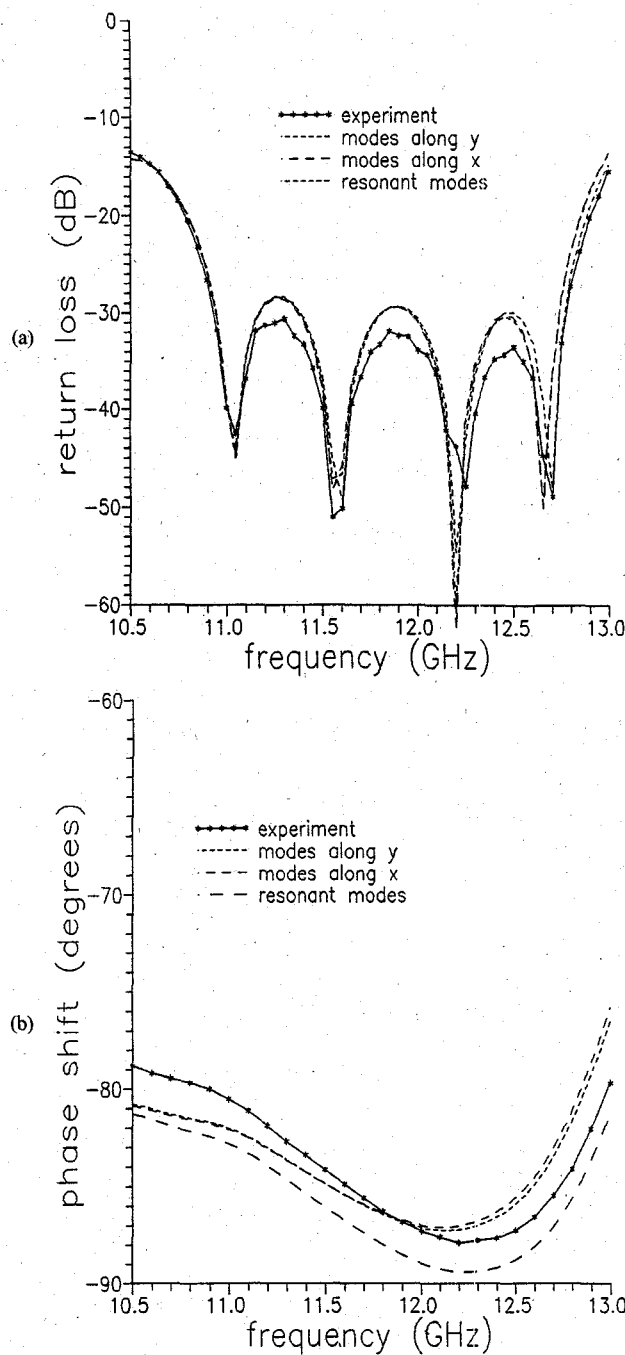


Fig. 15. Computed and measured responses of a 9-stub phase shifter.

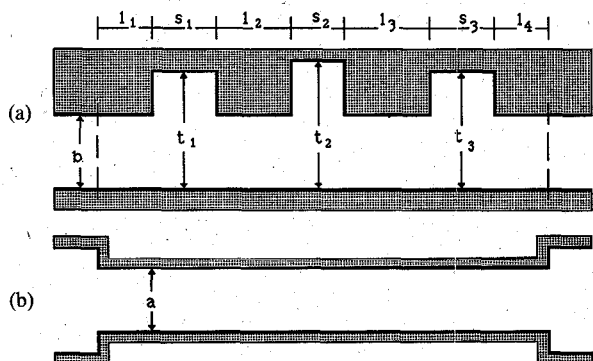


Fig. 16. Geometry of the phase shifter. E-plane (a) and H-plane (b) cross sections.

TABLE I  
DIMENSIONS (mm) OF A 9-CELL PHASE SHIFTER WITH SINGLE STUBS

$a = 16.639$	$b = 9.52$
$t_1 = t_9 = 13.785$	$t_2 = t_8 = 13.889$
$t_4 = t_6 = 13.893$	$t_5 = 13.615$
$l_1 = l_{10} = 11.615$	$l_2 = l_9 = 5.452$
$l_4 = l_7 = 4.710$	$l_3 = l_8 = 4.728$
$s_1 = s_9 = 2.989$	$s_2 = s_8 = 3.096$
$s_4 = s_6 = 3.106$	$s_3 = s_7 = 3.033$
$s_5 = 2.943$	

Ref. waveguide: WR75; Phase shift  $\Delta\phi_0$ :  $-85^\circ$ ; Length diff.  $\Delta L$ : 37.04 mm.

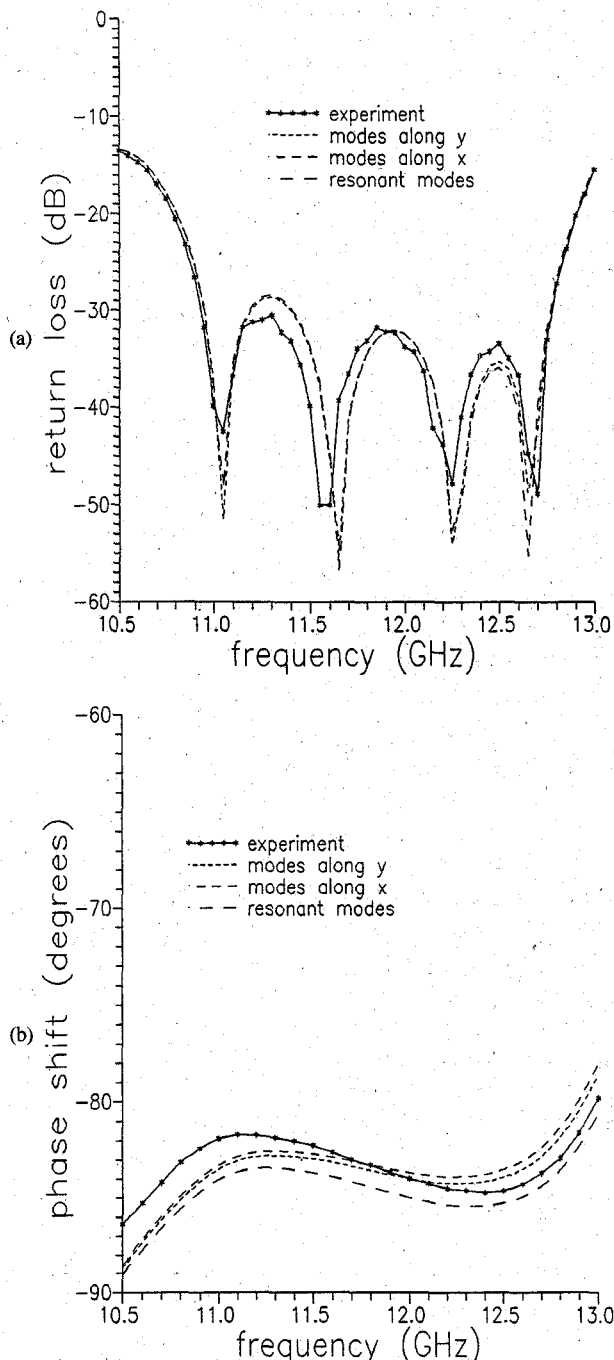


Fig. 17. Computed and measured responses of phase shifter with 6 double stubs.

TABLE II

DIMENSIONS (mm) OF A 6-CELL PHASE SHIFTER WITH SYMMETRICAL STUBS  
(DIMENSIONS ALONG  $y$  REFER TO ONE HALF OF THE ACTUAL STRUCTURE TO  
TAKE ADVANTAGE OF SYMMETRY)

$a = 16.08$	$b = 4.76$
$t_1 = t_6 = 7.97$	$t_2 = t_5 = 8.72$
$t_3 = t_4 = 8.26$	
$l_1 = l_6 = 10.80$	$l_2 = l_5 = 3.60$
$l_3 = l_4 = 3.68$	
$s_1 = s_6 = 494$	$s_2 = s_5 = 5.40$
	$s_3 = s_4 = 5.13$

Ref. waveguide: WR75; Phase shift  $\Delta\phi_o$ :  $-85^\circ$ ; Length diff.  $\Delta L$ : 37.04 mm.

Again, the three representations lead to quite close results, except that the numerical effort is drastically reduced using the representation in terms of modes propagating in the  $z$ -direction.

## VI. CONCLUSION

An efficient computer synthesis technique for waveguide components, based on rigorous field-theoretical models, has been presented and applied specifically to waveguide fixed phase shifters. The computer code developed requires only the electrical specifications to generate the geometrical structure of the components, in, usually, fifteen to twenty minutes on a 386/16 MHz IBM PC. The agreement with the experiments is so accurate as to avoid any tuning of the circuits realized.

The efficiency and accuracy of the technique is based on i) the adoption of a suitable segmentation technique of the microwave structure to obtain a very simple but rigorous network model; ii) the efficient representation of the modal series for the electromagnetic fields; iii) a synthesis procedure based on a simplified model to obtain a good initial guess for the final full-wave optimization routine.

Within the limits of validity of the planar circuit model [3], the technique can be applied with simple modifications to the synthesis of microstrip circuits.

## APPENDIX

The expressions for the generalized admittance matrix elements of a rectangular cell using the field expansion in terms of modes propagating along  $z$  (Fig. 3) are given in this Appendix. With the simplifications of Section III-B, the vector basis functions  $\phi_m^{(i)}$  have only the  $x$ -component, and can therefore be represented by scalar quantities.

Denoting with  $t_i$  the coordinate where the  $i$ th output port begins, and with  $w_i$  the width of this port, we have

$$\phi_m^{(i)} = C_m^{(i)} \cos \frac{(m-1)\pi(t-t_i)}{w_i}$$

where the index  $m$  is the order of the basis function and

$$C_m^{(i)} = \sqrt{\frac{\epsilon_m}{w_i}}$$

is the normalizing constant. The elements of the admittance matrix are given by

$${}_q Y_{mn}^{(i,j)} = j\omega\epsilon \int_{W_i} \int_{W_j} \phi_m^{(i)} {}_q G \phi_n^{(j)} dt dt' \quad (A1)$$

where  $q = o, y, z$ , and the corresponding expressions for  $G$  are given by (8), (10), and (11). Some particular expression of the admittance elements are given in the following with reference to the case  $q = z$ .

The admittance seen from port 1 corresponds to the admittance of a short-circuited section of waveguide of length  $c$  and is trivially given by

$${}_z Y_{mn}^{(1,1)} = j\omega\epsilon \frac{\epsilon_m}{b} \frac{\operatorname{ctg} k_{zm} c}{k_{zm}} \quad (A2)$$

where  $\epsilon_m = 1$  for  $m = 0$ ,  $\epsilon_m = 2$  for  $m \neq 0$ . The same expression (A2) would also result using  ${}_o G$ ,  ${}_y G$  instead of  ${}_z G$ , except the resulting single series has to be summed analytically to get the  $\operatorname{ctg}$  function.

The admittance between output port 1,  $N$  and output port  $j$  can be also expressed by just one term, namely

$${}_z Y_{mn}^{(1,j)} = j\omega\epsilon \sqrt{\frac{\epsilon_m}{b}} \frac{C_n^{(j)} J_{k_{zm} n}^{(j)}}{k_{zm} \sin k_{zm} c} \quad (A3)$$

with

$$J_{k_{zm} n}^{(j)} = \int_{z_j}^{z_j + w_j} \cos k_{zm}(c-z) \cos \frac{n\pi}{w_j}(z-z_j) dz \quad (A4)$$

easily evaluable analytically.

The admittance between two different output ports placed on the  $y = 0$  plane is given by a single, rapidly convergent series of the type

$${}_z Y_{mn}^{(i,j)} = j\omega\epsilon \sum_{m'=0}^{\infty} \frac{\epsilon_{m'} C_n^{(j)} C_m^{(i)}}{b} \frac{J_{k_{zm'} m}^{(j)} I_{k_{zm'} m}^{(i)}}{k_{zm'} \sin k_{zm} c} \quad (A5)$$

where we have also introduced

$$I_{k_{zm'} m}^{(i)} = \int_{z_i}^{z_i + w_i} \cos k_{zm'} z' \cos \frac{m\pi}{w_i}(z'-z_i) dz'$$

The fast convergence of (A5) is essentially due to the presence of the sine term, which, for large (imaginary) values of  $k_{zm} c$  behaves as an exponential.

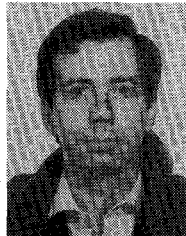
The mutual admittance between different modes  $m, n$  at the same physical output is given by

$${}_z Y_{np}^{(i,i)} = j\omega\epsilon \sum_{m=0}^{\infty} \frac{C_n^{(i)} C_p^{(i)} \epsilon_m}{b} \frac{(-1)^n \sin k_{zm}(z_i + w_i - c) I_{k_{zm'} p}^{(i)} - \sin k_{zm} z_i J_{k_{zm'} p}^{(i)} + \delta_{np} \frac{w_i}{\epsilon_n} \sin k_{zm} c}{\sin k_{zm} c \left[ k_{zm}^2 - \left( \frac{n\pi}{w_i} \right)^2 \right]} \quad (A6)$$

Observe that each term of the series (A6) is the sum of three terms. Because of the presence of the hyperbolic sine the first two terms converge very quickly. The remaining term can be easily summed by using the Contour-Integration method [16, p. 812].

## REFERENCES

- [1] K. C. Gupta *et al.*, *Computer-Aided Design of Microwave Circuits*. Dedham, MA: Artech House, 1981.
- [2] F. Alessandri, M. Mongiardo, and R. Sorrentino, "Computer-aided design of beam forming networks for modern satellite antennas," *IEEE Trans. Microwave Theory Tech.*, May 1992.
- [3] R. Sorrentino, "Planar circuits, waveguide models, and segmentation method," *IEEE Trans. Microwave Theory Tech.*, vol. MTT-33, pp. 1057-1066, Oct. 1985.
- [4] T. Okoshi, Y. Uehara, and T. Takeuchi, "The segmentation method—An approach to the analysis of microwave planar circuits," *IEEE Trans. Microwave Theory Tech.*, vol. MTT-24, pp. 662-668, 1976.
- [5] R. Chadha and K. C. Gupta, "Segmentation method using impedance matrices for analysis of planar microwave circuits," *IEEE Trans. Microwave Theory Tech.*, vol. MTT-29, pp. 71-74, 1981.
- [6] F. Alessandri, M. Mongiardo, and R. Sorrentino, "Transverse segmentation: a novel technique for the efficient CAD of 2N-Port branch guide couplers," *IEEE Microwave Guided Wave Lett.*, Aug. 1991.
- [7] J. Dittloff, F. Arndt, D. Grauerholtz, "Optimum design of waveguide E-plane stub-loaded phase shifters," *IEEE Trans. Microwave Theory Tech.*, vol. 36, no. 3, pp. 582-587, Mar. 1988.
- [8] F. Alessandri, M. Mongiardo, G. Schiavon, and R. Sorrentino, "Efficient computer aided design of wide-band stepped waveguide phase-shifters," in *Proc. 20th European Microwave Conf.*, Budapest, Sept. 1990, pp. 463-468.
- [9] V. P. Lyapin, V. S. Mikhalevsky, and G. P. Sinyavsky, "Taking into account the edge condition in the problem of diffraction waves on step discontinuity in plate waveguide," *IEEE Trans. Microwave Theory Tech.*, vol. MTT-30, pp. 1107-1109, July 1982.
- [10] C. Vassallo, "On a direct use of edge condition in modal analysis," *IEEE Trans. Microwave Theory Tech.*, vol. MTT-24, pp. 208-212, 1976.
- [11] T. Rozzi and M. Mongiardo, "E-plane steps in rectangular waveguide," *IEEE Trans. Microwave Theory Tech.*, vol. 39, no. 8, Aug. 1991.
- [12] R. Sorrentino, M. Mongiardo, F. Alessandri, and G. Schiavon, "An investigation on the numerical properties of the mode-matching technique," *Int. J. Numerical Modelling*, vol. 4, pp. 19-43, 1991.
- [13] C. G. Montgomery, R. H. Dicke, and E. M. Purcel, eds., *Principles of Microwave Circuits*, MIT Rad. Lab. Series, vol. 8, New York: McGraw-Hill, 1948. Reprinted by Peter Peregrinus on behalf of the Inst. Elec. Eng., 1987.
- [14] T. Itoh, "Generalized scattering matrix technique," T. Itoh, ed., in *Numerical Techniques for Microwave and Millimeter Wave Passive Structures*. New York: Wiley, 1989, ch. 10, pp. 622-636.
- [15] K. Kurokawa, *An Introduction to the Theory of Microwave Circuits*. New York: Academic Press, 1961, ch. 4.
- [16] R. E. Collin, *Field Theory of Guided Waves*. New York: IEEE Press, 1991, Sec. 2.18.
- [17] F. Alessandri, M. Mongiardo, and R. Sorrentino, "Synthesis of a class of waveguide phase shifters," in *Proc. 21st Eur. Microwave Conf.*, Stuttgart, 1991, pp. 321-326.
- [18] R. E. Collin, *Foundations for Microwave Engineering*. New York: McGraw-Hill, 1966, Ch. 8, p. 364 sgg.
- [19] F. Alessandri, G. Bartolucci, and R. Sorrentino, "Admittance-matrix formulation of waveguide discontinuity problems. Application to the design of branch-guide couplers," *IEEE Trans. Microwave Theory Tech.*, vol. 36, pp. 394-403, Feb. 1988.
- [20] P. M. Morse and H. Feshback, *Methods of Theoretical Physics*. New York: McGraw-Hill, 1950, pp. 1850-1851.
- [21] J. Bornemann and R. Vahldieck, "Characterization of a class of waveguide discontinuities using a modified  $TE_{mn}^x$  mode approach," *IEEE Trans. Microwave Theory Tech.*, vol. 38, no. 12, pp. 1816-1822, Dec. 1990.



**Ferdinando Alessandri** (M'91) graduated *cum laude* in electronic engineering from "La Sapienza" University of Rome, Rome, Italy, in 1986, with a thesis on the design of branch-guide directional couplers.

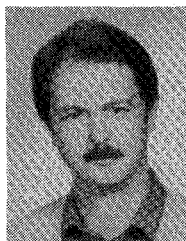
In 1989-90 he held a scholarship from the ASI (Italian Space Agency) working on satellite communication antennas. From 1990 to 1991 he was with Microdesign, Rome, working on the CAD of microwave beam forming networks. In 1992 he became a research assistant at the University of Perugia, Perugia, Italy. His research interests are in the area of numerical modeling of microwave and millimeterwave structures.



**Mauro Mongiardo** (M'91) received the Doctor degree in 1983 from the University of Rome "La Sapienza," and the Ph.D. from the University of Bath, Bath, U.K. in 1991.

He is currently at the University of Perugia, Perugia, Italy, on sabbatical from the University of Rome "Tor Vergata," Rome, where he is a research assistant. In 1988 he was a recipient of a NATO-CNR research scholarship during which he was a visiting researcher at the University of Bath. He is currently working in the modeling and com-

puter-aided design of microwave and millimeter wave guiding structures and antennas.



**Roberto Sorrentino** (M'77-SM'84-F'90) received the Doctor degree in Electronic Engineering from the University of Rome "La Sapienza," Rome, Italy, in 1971.

In 1971 he joined the Department of Electronics of the same University, where he became an Assistant Professor of Microwaves in 1974. He was also *Professore Incaricato* at the University of Catania, (1975-76), at the University of Ancona (1976-77), and at the University of Rome "La Sapienza" (1977-1982), where he then was an Associate Professor from 1982 to 1986. In 1983 and 1986 he was appointed as a Research Fellow at the University of Texas at Austin, Austin, USA. From 1986 to 1990 he was a Professor at the Second University of Rome "Tor Vergata." Since November 1990 he has been a Professor at the University of Perugia, Perugia, Italy. His research activities have been concerned with electromagnetic wave propagation in anisotropic media, interaction of electromagnetic fields with biological tissues, and mainly with the analysis and design of microwave and millimeter-wave passive circuits. He has contributed to the planar-circuit approach for the analysis of microstrip circuits and to the development of numerical techniques for the modeling of components in planar and quasi-planar configurations.

Dr. Sorrentino is a member of the editorial boards the IEEE TRANSACTIONS ON MICROWAVE THEORY AND TECHNIQUES, the *International Journal on Numerical Modelling*, the *International Journal of Microwave and Millimeter-Wave Computer-Aided Engineering* and of the *Journal of Electromagnetic Waves and Applications (JEWAA)*.